Case Report

Catalytic conversion of palm oil into sustainable biodiesel using rice straw ash supported-calcium oxide as a heterogeneous catalyst: Process simulation and techno-economic analysis

Phonsan Saetiao [a], Napaphat Kongrit [a], Chin Kui Cheng [b], Jakkrapong Jitjamnong [a,*], Chatrawee Direksilp [c], Nonlapan Khantikulanon [d]

[a] Petroleum Technology Program, Industrial Technology Department, Faculty of Industrial Education and Technology, Rajamangala University of Technology Srivijaya, 2/1 Rachadamnoennork Rd., Boryang, Muang, Songkhla 90000, Thailand
[b] Center for Catalysis and Separation, Department of Chemical Engineering, College of Engineering, Khalifa University, Abu Dhabi, United Arab Emirates
[c] Institute of Functional Interfaces (IFG), Karlsruhe Institute of Technology (KIT), Hermann-von-Helmholtz-Platz 1, 76344 Eggenstein-Leopoldshafen, Karlsruhe, Germany
[d] Department of Environmental Health, Faculty of Public Health, Valaya Alongkorn Rajabhat University Under the Royal Patronage, Khlong 1, Khlong Luang, Pathum Thani 10120, Thailand

A B S T R A C T

This study aimed to optimize the process parameters and evaluated economic feasibility for biodiesel production. A pyrolytic rice straw ash (RSA) support with various amounts of calcium oxide (25–35 wt%) and calcination temperatures (600–800 °C) were used in the study. The results identified 35 wt% of CaO/RSA and calcination at 600 °C as the most effective catalyst with turnover frequency (TOF) of 2.88 h^{-1} for biodiesel synthesis, giving a biodiesel yield of 96.49%. The optimal conditions for biodiesel production included a methanol: palm oil molar ratio of 9.34:1, a catalyst loading of 4.87 wt%, 175 min reaction time, and 65 °C reaction temperature. The study also included a techno-economic analysis of biodiesel production, revealing a payback period of 7.17 years, an internal rate of return of 17.20%, and a net present value of 4,151,905.61 USD. These findings pave the way for more sustainable and economically feasible biodiesel production.

1. Introduction

Currently, fossil fuels serve as the dominant energy source, representing more than 85% of the world's energy consumption. Nevertheless, the extensive combustion of these fuels results in the emission of greenhouse gases (GHGs), leading to climate change. The limited availability of fossil fuels and their adverse effects on the environment have sparked a worldwide interest in seeking sustainable and renewable alternatives to satisfy the continually growing energy requirements, which are estimated to reach 30 Terawatts by 2050 [1].

Biodiesel, derived from bio-oils obtained mainly from plants and their derivatives, is a renewable and perishable resource that offers several advantages over fossil fuels [2]. Unlike fossil fuels, which release harmful GHGs when burned, biodiesel is a clean-burning fuel that significantly reduces carbon dioxide, particulate matter, and sulfur emissions [3]. Typically, biodiesel is produced through transesterification, where the catalyst used plays a crucial role in the reaction's efficiency and sustainability. Catalysts can be either basic [4] or acidic [5], and can be homogeneous [6], heterogeneous [7], or bio-based [8]. While homogeneous catalysts, such as sodium hydroxide [6], potassium hydroxide [6], and sodium methoxide [9], are commonly used, they have some drawbacks that hinder their widespread adoption in sustainable biodiesel production.

A significant obstacle linked to homogeneous basic catalysts lies in their limited reusability. Furthermore, these catalysts are challenging to recover and reuse, leading to increased catalyst consumption and waste production [10]. In contrast, heterogeneous catalysts offer various benefits compared to their homogeneous counterparts. They can be easily retrieved from the reaction mixture using simple separation techniques like filtration or centrifugation, thereby reducing the necessity for additional purification steps. Additionally, heterogeneous catalysts can be recycled and utilized multiple times, resulting in lower

catalyst consumption and decreased waste generation [11,12].

Sustainable development has become a critical global goal, and finding innovative ways to repurpose waste materials is a key aspect of achieving this objective. The use of biochar and ash catalysts for biodiesel production offers several benefits beyond their catalytic performance. These materials are derived from waste biomass, which can help to reduce the environmental burden associated with waste disposal. Moreover, their low cost and abundance make them attractive alternatives to conventional catalysts, which are often expensive and derived from non-renewable resources [13]. Rice straw (RS), the leftover stalks and stems after rice harvesting is a waste material that is often burned in open fields, contributing to environmental pollution and health hazards. However, recent advancements in technology and research have unlocked the potential of RS as a valuable feedstock for biofuel production, offering significant environmental and economic benefits [14].

In today's competitive business landscape, optimizing manufacturing processes is crucial for companies to stay ahead. With the increasing complexity of software systems, finding ways to improve performance while minimizing resource requirements has become a top priority. One essential tool that can aid in this endeavor is techno-economic analysis (TEA). A TEA allows companies to assess the economic feasibility of their industrial processes by considering the material balance of various process streams and generating valuable simulation data [15]. Moreover, TEA provides a comprehensive view of the costs and benefits associated with a process, taking into account factors such as raw material costs, utilities, labor, and equipment. This economic analysis enables companies to make informed decisions about the viability of their operations and identify areas for improvement. Additionally, TEA includes a profitability analysis that assesses the revenues generated not only by the main product but also by any by-products, providing a holistic picture of the financial performance of the process. One promising application of TEA is in the field of biodiesel production. Recent studies have proposed novel methods for producing biodiesel using heterogeneous catalysts that hold potential for improving the efficiency and sustainability of biodiesel production, and TEA can play a vital role in evaluating their economic viability [16]. The existing literature indicates a significant research gap pertaining to the utilization of CaO/RSA as a heterogeneous catalyst in the transesterification process and its economic feasibility for biodiesel production. To bridge this gap, the authors have undertaken this study with the specific objective of addressing and exploring.

The aim of this research was to develop a novel catalyst system for sustainable biodiesel production. The catalyst was derived from the pyrolysis of RS to form a RS ash (RSA) support and subsequently loaded with different CaO levels loading catalysts and calcination temperatures to form the basic heterogeneous catalysts. The optimal operational parameters for the synthesis of biodiesel were evaluated by utilizing response surface methodology (RSM). The economic viability of this breakthrough catalyst system was then studied and sensitivity analysis was conducted to assess the impact of raw material costs and biodiesel prices on the overall production cost.

2. Materials and methods

2.1. Materials

The RS was obtained from Songkhla province, Thailand. Refined palm oil (RPO), purchased from a local supermarket in Thailand, and was used as the starting material for biodiesel production. The chemical composition of the feed RPO was determined using thin layer chromatography/flame ionization detection. The results revealed that the triglyceride content was 98.57 wt%, while the diglyceride and monoglyceride contents were 1.37 wt% and 0.06 wt%, respectively. Commercial CaO was selected as an alkaline promoter for the transesterification process. Methanol of analytical reagent grade was used as a reactant and was sourced from RCI Labscan Limited.

2.2. Catalyst preparation

The RS samples were thoroughly washed with distilled water to remove impurities from the surface. The samples were dried at 105 °C overnight and ground into a fine powder. The dried RS powder was calcined at 800 °C for 4 h under atmospheric pressure, using a heating rate of 10 °C/min. The obtained RSA as then activated by stirring it in a 2 M KOH solution for 2 h, filtered, and then the filtrate was washed with distilled water several times until its pH value reached 7. The obtained RSA was dried in an oven at 105 °C overnight.

The dried RSA was mixed with CaO using the wet impregnation method, varying the concentration of CaO between 25 and 35 wt%. In a typical process for preparing a catalyst with 30 wt% CaO loading, 3 g of CaO powder was added to 100 mL of distilled water, and 7 g of dried RSA was added to the solution. The mixture was then stirred for 2 h to ensure thorough mixing. After stirring, the sample was dried in an oven at 105 °C for 24 h. Subsequently, it was calcined at different temperatures ranging from 600 °C to 800 °C under atmospheric pressure for 4 h. The resulting catalysts were labeled as xCaO-RSA-T, where x represents the CaO loading level (wt.%) and T represents the activation temperature.

2.3. Catalyst characterization

The surface morphology and elemental composition of each catalyst was evaluated using scanning electron microscopy (SEM; Oxford Aztec model) equipped with an energy dispersive spectroscopy (EDS) detector. Solid powders were placed on SEM holders and coated with a thin layer of gold. Analysis was conducted at magnifications of 50 and 1000 times, with an accelerating voltage of 10 kV.

The basic strength of the prepared catalysts was assessed using Hammett indicators method. The indicators, including bromothymol blue (H_- = 7.2), phenolphthalein (H_- = 9.8), 2,4-dinitroaniline (H_- = 15.0), and 4-nitroaniline (H_- = 18.4), were used. The catalysts' total basicity was determined by titrating with a benzoic acid solution (0.01 M) dissolved in anhydrous methanol, which served as the titrant.

The chemical composition of each catalyst was determined using wide angle X-ray diffractometry (XRD; Rigaku). The catalyst was pressed onto glass sample holders specifically designed for XRD measurements. The XRD analysis was conducted using Cu-Kα radiation with a wavelength (λ) of 0.15405 nm, generated by a 2.2 kW Cu anode and a fine focus ceramic X-ray tube. The measurements were carried out at a temperature of 25 °C, with a 2θ scanning range between 10 and 90°. The scanning speed was set at 5° min^{-1}, and the scan step was kept at 0.02° to ensure accurate results. The average diameter of crystalline size, denoted by D, can be determined using the Debye-Scherrer relation, as given by Eq. (1):

$$D = 0.9 * \lambda / \beta * \cos(\theta) \tag{1}$$

Where λ represents the wavelength of CuKα radiation at 0.154 nm, β denotes the half maximum intensity, which represents the broadening of the diffraction peaks due to the size of the crystalline grains, and θ is the Bragg angle, which is the angle at which the diffraction peaks occur during X-ray diffraction analysis.

The elemental analysis of each catalyst was ascertained using X-ray photoelectron spectrometry (XPS; Kratos, Axis Ultra DLD, Manchester, UK). The XPS analysis was carried out with monochromatic Al Kα radiation as the radiation source, operating under high vacuum at 15 kV. Survey and high-resolution scans were recorded with analyser pass energies of 160 and 40 eV, respectively. To ensure accurate calibration, the C 1s peak at 284.8 eV was utilized as a reference for all XPS spectra. Interpretation of the XPS spectra was performed using Casa XPS software.

2.4. Experimental design for transesterification and statistical analysis by RSM

The biodiesel production process was optimized using RSM, a statistical technique commonly used for process optimization in various fields, with trials conducted using Design Expert version 13 software (Stat-Ease Inc., Minneapolis, MN, USA). To design the experiments, a five-level central composite design (CCD) with six replicate points at the central point was utilized (see supplementary material). The design incorporated combinations of experiments with axial points (2k), factorial points (2^k), and center points (no = 6). The total number of experiments (N) in the CCD design was determined by summing the axial points, factorial points, and center points, as expressed in Eq. (2):

$$N = 2^k + 2k + 6 \qquad (2)$$

The obtained data from the experimental runs were analyzed, as shown in Eq. (3), which was employed for the final analysis using RSM:

$$Y = \beta_0 + \beta_1 A + \beta_2 B + \beta_3 C + \beta_{12} AB + \beta_{13} AC + \beta_{23} BC + \beta_{11} A^2 + \beta_{22} B^2 + \beta_{33} C^2 \qquad (3)$$

Where Y represents the predicted biodiesel yield, which is the main component of biodiesel. The coefficients β_0, β_1, and β_2 represent the main effects of the respective input variables (A, B, and C) on the response variable. The coefficients β_{12}, β_{13}, and β_{23} represent the interactive effects of two variables, and the coefficients β_{11}, β_{22}, and β_{33} represent the quadratic effects of the respective variables. The RSM analysis was applied to systematically evaluate the impact of individual reaction parameters and their combinations on biodiesel yield. The statistical significance of the model was determined using p-values, while additional metrics such as the F-test, coefficient of determination (R^2), predicted R^2, and adjusted R^2 were examined to ensure the reliability.

2.5. Transesterification reaction

In this process, 50 g of RPO was added to a three-necked round-bottom flask and heated to 65 °C in an oil bath. In a separate beaker, a blend was prepared by combining the desired amount of methanol to achieve the desired methanol: RPO molar ratio (ranging from 3:1 to 15:1) and the catalyst (ranging from 3 to 7 wt% compared to RPO) at room temperature. The blend was then decanted into the preheated RPO in the flask and brought to the selected reaction temperature. Once the desired reaction temperature was reached, the mixture was maintained with stirring at 500 rpm under reflux condensation for various times (ranging from 120 to 240 min). The mixture was filtered to remove the catalyst. The resulting filtrate was then kept in a funnel separator for 24 h. The upper layer, which contained fatty acid methyl esters (FAME), was washed with distilled water at 60 °C multiple times until the pH reached 7, in order to remove excess methanol, glycerol, and alkali. Finally, the obtained FAME was stored in a glass bottle containing anhydrous sodium sulfate to remove any adsorbed moisture. The biodiesel yield was determined using Eq. (4):

$$\text{Biodiesel yield (\%)} = \frac{Weight\ of\ biodiesel\ produced}{Weight\ of\ starting\ palm\ oil\ used} \times 100 \qquad (4)$$

In order to assess the reusability of the catalyst, a post-transesterification reaction evaluation was conducted. To ensure that the catalyst could be reused effectively, a thorough methanol wash was performed to eliminate any potential residue. After the wash, the catalyst was then dried overnight in an oven set at 105 °C in preparation for the subsequent run.

2.6. Biodiesel analysis

The optimal conditions for characterizing RPO-derived FAME were determined using gas chromatography (GC) with a Hewlett-Packard 5890 Series II equipped with a FID. The DB-WAX column used had a film thickness of 0.2 μm. The helium gas flowed at a rate of 70 mL/min. The injector and detector temperatures were set at 200 °C with a split ratio of 75:1, and 230 °C, respectively. The total running time of the analysis was 62.5 min [17].

2.7. Process design of biodiesel production

Triolein ($C_{57}H_{98}O_6$) and methyl oleate ($C_{19}H_{36}O_2$) were employed as model compounds to represent the RPO and the transesterification product, respectively. The preliminary design of the process was carried out using Aspen Plus V11. The thermodynamic modeling employed the non-random two liquid model, which utilized binary interaction parameters derived from a previous study [18]. This model facilitated the prediction of vapor-liquid equilibrium and liquid-liquid equilibrium in the system.

For the small-scale biodiesel plant, several assumptions were made. The objective of this project was to develop a biodiesel production capacity of 10,000 tons per year. The specification included the use of commercial-grade pure triolein and achieving a biodiesel purity of 99.992%. The design of the reactions was based on reaction conversion and stoichiometric balance. Continuous oil feeding throughout the year was assumed. The simulation of the process utilized optimized results obtained from lab-scale experimental data. Vacuum distillation was employed to maintain the temperature below 275 °C, thereby preventing biodiesel degradation.

2.8. Economic feasability: TEA

The TEA simulations are an important tool for determining the feasibility and profitability of industrial projects. The TEA simulation, using data from lab-scale optimization was used to plan the construction of a RPO-biodiesel production plant. The simulation took into account a construction period of 24 months, a start-up period of 12 months, and a projected lifetime of 20 years. To ensure efficient operation of a RPO-biodiesel production plant, it is crucial to estimate the required number of operators accurately. In a recent study, a formula (Eq. 5) was used to estimate the number of operators required (N_{OL}) for the plant based on the total number of particulate handling unit operations (P) and non-particulate handling unit operations (N_{np}),

$$N_{OL} = (6.29 + 31.7P^2 + 0.23N_{np})^{0.5} \qquad (5)$$

The plant was designed to operate for 50 weeks per year, with 5 shifts per week per person and 3 shifts per day. This calculation takes into account the deduction of sick and vacation days from the total of 52 weeks in a year.

In the economic analysis of project investments, one commonly used metric to determine profitability is the internal rate of return (IRR). A high IRR suggests that the project was more profitable and sustainable. The formula used to calculate the net present value (NPV) takes into account the discounted cash inflow and initial cash outlay, as represented in Eq. (6). The IRR is calculated when the discounted cash inflow and initial cash outlay equal zero [19], as shown in Eq. (7).

$$NPV = \sum_{t=0}^{n} \frac{R_t}{(1+i)^t} \qquad (6)$$

where the NPV of the project is represented by NPV, t shows the year of operation, R_t represents delta the cash inflow and cash outflow over period t, and i presents the discount rate.

$$NPV = 0 = \sum_{t=1}^{n} \frac{C_t}{(1+IRR)^t} C_o \qquad (7)$$

where t denotes the number of time periods; C_t shows the net cash inflows generated by the investment project; and C_0 presents total initial

Table 1
Economic assumptions for the cost of raw materials, products, and utilities.

Detail	Cost	Reference
Materials		
Oil	0.255 USD/kg	[23]
Methanol	0.23 USD/kg	[19]
Catalyst	0.120 USD/kg	[24]
Product		
FAME	1.0 USD/kg	[25]
Glycerol	0.265 USD/kg	[26]
Utilities		
Steam (120 °C), LPS	7.05 USD/GJ	[21]
Steam (184 °C), MPS	8.22 USD/GJ	[21]
Steam (350 °C), HPS	14.62 USD/GJ	[21]
Cooling water	0.354 USD/GJ	[21]
Chilled water	4.43 USD/GJ	[21]
Electricity	0.1 USD/kWh	[22]

investment costs.

The payback period (PBP) is a metric used to determine the total time required to recover the capital investment of a project [19]. It can be calculated using Eq. (8),

$$PBP = \frac{Cost\ in\ investment}{Annual\ net\ cash\ flow} \tag{8}$$

2.8.1. Total capital investment (TCI) assumptions

Undertaking a large-scale industrial project requires a thorough understanding of the costs involved, particularly the TCI. The TCI is the sum of fixed capital investment (FCI) and working capital investment (WCI), for which a work-based calculation to provide an overview of capital investment assumptions was provided previously [20]. The FCI is composed of two parts: the total direct cost (TDC) and the total indirect cost (TIC). The TDC includes several costs, such as the purchased equipment cost (PEC), land, buildings, process and auxiliary costs, equipment installation and painting, instrumentation and controls, piping, electrical systems, and service facilities and yard improvements. On the other hand, the TIC includes several costs, such as engineering and supervision costs, legal expenses, construction expenses, constructor's fees, and contingency charges.

2.8.2. Assumptions in the total production cost (TPC)

The TPC is a crucial factor for any manufacturing operation and is composed of four primary cost components: direct production, fixed charges, plant overhead, and general expenses (GE), and can be calculated based on work-related factors [20]. Direct production costs encompass raw materials (C_{RM}), utilities (C_{UT}) (Table 1), operating labor (C_{OL}), waste treatment, and maintenance and repairs. Fixed charges include insurance and local taxes. Plant overhead is a general cost category that encompasses all other expenses associated with operating the production facility. The GE includes research and development, distribution and marketing, and administrative costs. These costs are not directly related to the production process but are necessary for the successful operation of the business.

3. Results and discussion

3.1. Catalyst characterization

The surface properties of RSA and 35CaO/RSA-600 were determined from the SEM images. The RSA catalyst had a systematic and undamaged surface, but it had an uneven surface and an amorphous structure, which could be attributed to lignin coverage on the fibers [21]. Upon activation with 35 wt% CaO and calcination at 600 °C, the resulting catalyst then exhibited an irregular particle shape due to the CaO compounds covering the surface of the RSA (see supplementary material). This irregularity was due to the low carbon content and lignin

solubilisation of RS, which resulted in small surface cavities and an increased surface area [22,23].

The EDS analysis revealed that the RSA catalyst primarily consisted of carbon, oxygen, silicon, and potassium, with trace amounts of magnesium (see supplementary material). In contrast, the 35CaO/RSA-600 catalyst showed a significant increase in the calcium content (42.0 wt %) compared to the RSA catalyst, indicating the successful incorporation of CaO into the catalyst. The major components of the catalysts were calcium, silica, magnesium, and potassium, mostly present in the form of oxides due to the high oxygen content.

The broad diffraction peak observed at a 2θ of 10–30° in the RSA catalyst is attributed to amorphous carbon, which is a form of carbon that lacks a regular crystalline structure (see supplementary material). Additional peaks at a 2θ of 20.53°, 27.64°, and 42.68° were observed, which correspond to the SiO_2 phase, indicating the presence of SiO_2 in the catalyst [24,25], a common compound found in many natural materials. Its presence in the catalyst suggests that it may play a role in the catalyst's performance. Furthermore, the RSA catalyst exhibited peaks at a 2θ of 29.02° and 39.76°, which are attributed to the presence of potassium chloride (KCl), which can form during the combustion process [25]. After loading of CaO species, the XRD analysis revealed clear diffraction peaks at a 2θ of 29.30°, 32.22°, 35.96°, 37.28°, 47.16°, and 64.64°, which were attributed to the presence of CaO [4,26–28]. This indicated that CaO species were successfully loaded onto the catalyst.

Interestingly, the crystalline phase of Ca_2SiO_4 has been observed in catalysts with different CaO loadings and temperatures. The 2θ values of the Ca_2SiO_4 crystalline phase were found at 31.22°, 31.32°, 31.57°, and 31.23° for catalysts with increasing CaO loadings of 25CaO/RSA-600, 30CaO/RSA-600, 35CaO/RSA-600, and 35CaO/RSA-700, respectively [29]. This observation confirms the successful reaction of CaO with SiO_2, leading to the formation of Ca_2SiO_4. Interestingly, as the CaO loading increased from 25 to 35 wt% and with a 600 °C calcination temperature, the 2θ values of the Ca_2SiO_4 crystalline phase shifted to higher angles, suggesting a change in the crystalline structure. This indicates that a higher amount of CaO may promote the formation of a more stable and well-defined Ca_2SiO_4 crystalline phase, leading to an enhanced catalyst performance. Furthermore, when the 35CaO/RSA catalyst was subjected to a calcination temperature of 800 °C, the Ca_2SiO_4 crystalline phase disappeared, indicating that the temperature plays a critical role in the stability of the Ca_2SiO_4 phase, and at high temperatures, the phase can undergo structural changes or decompose, leading to the disappearance of the crystalline phase.

The basic strength and total basicity of synthesized solid base heterogeneous catalysts were measured using the Hammett indicators method (see supplementary material). The RSA had a low basic strength (7.2 < H_) and total basicity (1.80 mmol/g) due to its slight alkaline content, which made it unsuitable for catalyzing the transesterification reaction. However, loading RSA with CaO (from 0 to 35 wt%) significantly increased the base strength and total basicity of the synthesized catalysts. The 25CaO/RSA-600, 30CaO/RSA-600, 35CaO/RSA-600, 35CaO/RSA-700, and 35CaO/RSA-800 samples showed basic strengths ranging from 9.8 to 15.0 and a total basicity ranging from 7.10 to 8.69 mmol/g, increasing with higher CaO loading levels, and so had a higher basic strength and total basicity compared to RSA, making them more effective in enhancing the transesterification catalytic activity of RPO/methanol into biodiesel. The TOF is a critical parameter used to assess the effectiveness of heterogeneous catalysts in biodiesel synthesis. The TOF was calculated using Eq. (9), and it was found to be 2.88 h^{-1}. However, Basumatary et al. [30] reported a TOF of 6.59 h^{-1} in their biodiesel synthesis study, where they utilized a solid catalyst derived from sugarcane bagasse ash. Furthermore, in another study by Basumatary et al. [31] focusing on biodiesel synthesis with a *Heteropanax fragrans* ash solid catalyst, an even lower TOF of 0.59 h^{-1} was observed.

$$Turnover\ frequency\ (TOF)\ h^{-1} = \frac{Biodiesel\ produced\ (mol)}{Basicity\ x\ 0.001\ (mol)\ x\ time\ (h)} \tag{9}$$

Table 2

Actual and predicted values of response surface analysis for biodiesel production using 35CaO/RSA-600 as heterogeneous catalyst.

Run	Methanol: oil molar ratio (A)	Catalyst loading (wt.%) (B)	Reaction time (min) (C)	Observed FAME yield (%)	Predicted FAME yield (%)
1	12:1	6	210	68.67	68.69
2	9:1	5	180	97.36	97.18
3	12:1	6	150	89.94	88.44
4	3:1	5	180	72.40	69.34
5	9:1	5	180	96.45	97.18
6	9:1	3	180	89.94	87.90
7	9:1	5	120	71.94	72.24
8	9:1	5	180	96.21	97.18
9	12:1	4	210	75.21	76.05
10	9:1	5	180	98.39	97.18
11	9:1	5	180	98.27	97.18
12	12:1	4	150	89.94	89.88
13	9:1	5	240	67.03	64.91
14	6:1	4	150	71.60	73.39
15	15:1	5	180	69.20	70.45
16	6:1	6	150	76.60	77.57
17	9:1	7	180	84.50	84.72
18	6:1	6	210	82.20	84.07
19	9:1	5	180	98.20	97.18
20	6:1	4	210	82.50	85.81

Table 3

Fit summary statistics for model prediction.

Source	Sequential p-value	Adjusted R^2	Predicted R^2	Remark
Linear	0.9335	−0.1568	−0.5027	
Interactive (2FI)	0.5204	−0.2040	0.5569	
Quadratic	<0.0001	0.9648	0.8603	Suggested
Cubic	0.1361	0.9789	0.0104	Aliased

The particle size of the catalyst was determined using the Debye-Scherrer method. For RSA, the particle size was determined to be 4.61 nm (see supplementary material). However, when CaO was loaded onto the RSA at various calcination temperatures, the particle size of the resulting catalysts varied significantly. The 35CaO/RSA-600 catalyst had the largest particle size of 38.75 nm, larger than in the 30CaO/RSA-600 catalyst, and increasing the calcination temperature to 700 °C and 800 °C resulted in the particle size of the 35CaO/RSA catalyst decreasing to 33.69 nm and 29.57 nm, respectively. Thus, the CaO loading level and calcination temperature have a substantial influence on the particle size of RSA-derived catalysts.

The XPS analysis revealed that the surface of RSA and the fractionated samples contained various elements, including carbon, oxygen, potassium, and silicon (see supplementary material). Carbon was the major component, comprising 59% of the total element content. The presence of aliphatic and aromatic carbons of lignin in RSA was attributed to this finding, which was confirmed by the EDS analysis. The high-resolution C1s spectrum showed peaks at 284.75–288.68 eV, corresponding to carbon linked to carbon (C–C) or hydrogen (C–H) groups in the aliphatic and aromatic carbons of lignin present on the exterior surface of the RS [32]. The O1s spectrum revealed peaks at 531.52–533.47 eV, indicating the presence of C–O and O–C═O functional groups, mainly originating from lignin [33]. The Si2p spectrum showed a primary peak centered at 103.45–103.96 eV, indicating the existence of Si–C, SiOx, and Si–O–Si [32]. Upon the addition of CaO to RSA, the C1s peak in the wide scan mode decreased from 59 to 38.37%, which reflected the removal of lignin during the during modification process. Previous studies have demonstrated that alkali treatments, like the addition of CaO, can disrupt hydrogen bonds within the complex lignocellulose structure, leading to the exposure of lignin and hemicelluloses on the surface [34]. The binding energy (BE) values of C1s,

O1s, and Si2p were slightly shifted to lower values, indicating electron transfer from Ca to other species. Based on the Ca2p BE value, the Ca species strongly interacted with Si and/or O species to create functional groups, such as CaO and/or Ca_2SiO_4, that effectively anchored on the surface of the 35CaO/RSA-600 catalyst and could act as active sites for the transesterification reaction.

3.2. Influence of the CaO loading level on the catalytic performance

The initial yield of biodiesel over the RSA catalyst was quite low at 8.50% (see supplementary material). However, the catalytic activity of the RSA catalyst increased significantly when increasing the CaO loading level up to the optimal level. In fact, as the CaO loading increased from 25% to 35%, the catalytic activity rose from 90.67% to an impressive 97.48%. Thus, increasing the CaO loading beyond a certain point may not necessarily result in a significant improvement in the catalytic activity of the RSA catalyst for biodiesel production. The RSA catalyst had a very low basicity, while the 35 wt% CaO loaded catalyst exhibited the strongest basicity. This suggests that the high biodiesel yield was due to the strong basicity of the catalyst with CaO loading and that the CaO loading level plays a crucial role in determining the catalytic activity of the catalyst in biodiesel production. Based on these findings, the study determined that the optimal CaO loading level for the RSA catalyst was 35 wt%.

3.3. Influence of the calcination temperature on the catalytic performance

The results showed that as the calcination temperature was increased to 600 °C, the yield of biodiesel production increased significantly to 97.48% (see supplementary material). This can be attributed to the formation of new CaO and Ca_2SiO_4, resulting in a stronger basicity at elevated temperatures. Among all the catalysts studied, 35CaO/RSA-600 exhibited the highest basicity of 8.69 mmol/g, while the lowest basicity was recorded for 35CaO/RSA-800 at 7.10 mmol/g. This decrease in basicity could be linked to the formation of CaO crystals and sintering of CaO particles at high temperatures, resulting in the weaker basicity. Thus, increasing the calcination temperature may not necessarily result in significant improvements in the catalytic activity of CaO for biodiesel production and careful consideration must be given to the temperature range used to optimize the process. In this study, the optimal CaO loading level for the RSA catalyst was 35 wt% with a calcination temperature of 600 °C.

3.4. Optimization of biodiesel production process by RSM

The study utilized a CCD to investigate the effects of three parameters: methanol: RPO molar ratio, catalyst loading level, and reaction time. The experiment involved 20 runs and was carried out using the 35CaO/RSA-600 catalyst. Six replicates of the reaction were run at the central point, which yielded an average biodiesel yield of 97.48 ± 0.97%. The regression equation and statistical analysis were obtained using Design Expert software based on the parameters used in the experiment. The quadratic polynomial equation developed from the study is shown in Eq. (10):

$$\text{Biodiesel yield (\%)} = 98.18 + 0.2787A - 0.7950B - 1.83C - 1.40AB - 6.56AC - 1.48BC - 6.82A^2 - 2.72B^2 - 7.15C^2 \tag{10}$$

The methanol: RPO molar ratio (A) had a positive impact on the biodiesel yield, while the remaining parameters had a negative impact. Equation (9) was then used to predict the biodiesel yield and to subsequently compare it to the obtained biodiesel yield from the experimental runs (Table 2). The biodiesel yield was found to be in the range of 67.03%–98.39%.

Comparison of sequential model fitting methods, focusing on the sequential model sum of squares and coefficient of determination was

Table 4
ANOVA of the quadratic model for biodiesel production using 35CaO/RSA-600 as heterogeneous catalyst.

Source	Sum of Squares	df	Mean Square	F-Value	p-Value
Model	2467.22	9	274.14	58.94	<0.0001
A-Methanol: oil molar ratio	1.24	1	1.24	0.2673	0.6164
B-Catalyst loading (wt.%)	10.11	1	10.11	2.17	0.1711
C-Reaction time (min)	53.73	1	53.73	11.55	0.0068
AB	15.79	1	15.79	3.40	0.0952
AC	344.53	1	344.53	74.07	<0.0001
BC	17.52	1	17.52	3.77	0.0810
A^2	1169.88	1	1169.88	251.52	<0.0001
B^2	185.50	1	185.50	39.88	<0.0001
C^2	1285.37	1	1285.37	276.35	<0.0001

performed for four polynomial models - linear, interactive (2FI), quadratic, and cubic models - to determine the best fit for the biodiesel yield (Table 3). The quadratic model demonstrated the best statistical fit for biodiesel yield when using the 35CaO/RSA-600 catalyst. Consequently, this model was selected for further statistical studies.

The effectiveness of a quadratic model for predicting the biodiesel yield was investigated through ANOVA analysis (Table 4), revealing that the quadratic model was statistically significant at a confidence level of 95%, with a low p-value of less than 0.001. Furthermore, the reaction time, interaction between the methanol: RPO molar ratio and reaction time, and all the quadratic terms were all significant (p-value below 0.05). The mean performance characteristics were analyzed, and Fischer's test value (F-value) was used to determine the model's significance. The F-value (58.94) for the model was significant, indicating that the model was effective in optimizing the transesterification process. Furthermore, there was only a 0.01% chance of the value being due to noise, indicating that the model's effectiveness was not coincidental. As a result, the transesterification of RPO using the 35CaO/RSA-600 catalyst within the designated process parameter levels was a proven success. The coefficient of determination (R^2) and adjusted R^2 were also calculated to assess the correlation between actual and predicted values, and found to be close to 1.0 (0.9815 and 0.9648, respectively), indicating an excellent correlation between the two sets of values and further supporting the efficacy of the model for predicting the biodiesel yield [35].

The predicted values and actual experimental results of the transesterification processes revealed the relationship between the responses and biodiesel yield (see supplementary material), and the optimal conditions for achieving the maximum biodiesel yield. The points on the graph are closely aligned with the line of perfect fit, indicating a minimal error of distribution. The externally studentized residuals plot was used to assess the fitness of the model. All the data points lied within a ± 4 limit (see supplementary material), indicating that the model is a good fit for the data and that there are no significant outliers or influential points. Thus, the model accurately captures the relationship between the variables under consideration. The normal % probability plot of residuals was used to assess whether the residuals were normally distributed and whether there was any deviation in the variance (see supplementary material). The residuals were constantly distributed and laid close to a straight line. This indicates that there was no deviation in the variance, and the model is a good fit for the data.

Perturbation plots exhibited that the reaction time had the most significant impact on the biodiesel yield, followed by the catalyst loading level (see supplementary material). Therefore, perturbation plots can serve as a useful tool for identifying the order of each process variable and its effect on the biodiesel yield.

3.5. Interaction effect of the process parameters on the biodiesel yield: a RSM approach

The study focused on using the 35CaO/RSA-600 catalyst since it demonstrated superior catalytic performance compared to the other catalysts (sections 3.2–3.4).

3.5.1. Interactive effect between methanol: RPO molar ratio and the catalyst loading

Fig. 1A and B shows the experimental results for changes in the methanol: RPO molar ratio (ranging from 3:1 to 15:1) and catalyst loading (varied between 3 and 7 wt%) on the biodiesel yield while maintaining a constant reaction time of 180 min. Increasing the methanol: RPO molar ratio and catalyst loading had a positive effect on the biodiesel yield, with the highest yield (98.2%) obtained with a methanol: RPO molar ratio of 9:1 and a catalyst loading of 5 wt%. This increased efficiency in the biodiesel production was attributed to the formation of methoxide ions in the liquid mixture. These ions act as a breaking agent for carbonyl bonds to alkyl esters, which improves the chemical reaction kinetics during the transesterification process [12]. The reacted methoxide acts as a promoter on the transesterification process, thereby optimizing the efficiency of the process [36]. However, further increasing the methanol: RPO molar ratio up to 15:1 at a catalyst loading of 5 wt%, led to a decreased biodiesel yield to 69.2%. This decrease is attributed to the reversible reaction resulting from the increased interaction between dissolved reactants [37]. The yield of biodiesel was significantly influenced by the amount of catalyst used in the process, where increasing the catalyst loading from 3 wt% to 5 wt% led to an increase in the biodiesel yield from 89.94% to 98.20%, a trend that is comparable to the effect of the methanol: RPO molar ratio. However, further increasing the catalyst loading beyond 5 wt% decreased the biodiesel yield due to the elevated viscosity of the reactants that then led to an increased mass transfer resistance in the reaction system [12]. According to the ANOVA results, there was no significant interaction effect between the methanol: RPO molar ratio and catalyst loading in the chemical process being studied.

3.5.2. Interactive effect between the methanol: RPO molar ratio and reaction time

Fig. 1C, D illustrates the relationship between the methanol: RPO molar ratio and reaction time on the biodiesel yield under a constant catalyst loading of 5 wt%. The highest biodiesel yield (over 98.20%) was obtained at a methanol: RPO molar ratio of 9:1 and a reaction time of 180 min. Interestingly, increasing the methanol: RPO molar ratio beyond 9:1 did not result in any substantial improvement in the biodiesel yield, but rather decreased it at methanol: RPO molar ratios above 9:1.

The biodiesel yield increased as the reaction time increased from 120 min to 180 min, but further increasing the reaction time up to 240 min, in combination with a methanol: RPO molar ratio of 9:1, decreased the biodiesel yield to 67.03%. This was attributed to the high viscosity of the mixture, making it difficult for biodiesel separation, and the occurrence of the saponification reaction [38]. The reaction time had the highest ANOVA F value, implying that it was the most influential parameter on the biodiesel yield in the chemical process being examined, while the combined effect of the methanol: RPO molar ratio and reaction time was statistically significant.

3.5.3. Interactive effect between the catalyst loading level and the reaction time

Fig. 1E, F presents the impact of the catalyst loading and reaction time on the biodiesel yield, with a fixed methanol: RPO molar ratio of 9:1. Increasing the catalyst loading and reaction time up to the optimal values improved the biodiesel yield. A catalyst loading of less than 5 wt% led to less than 90% biodiesel yield throughout the 180 min reaction time, but a catalyst loading of 5 wt% and a reaction time of 180 min
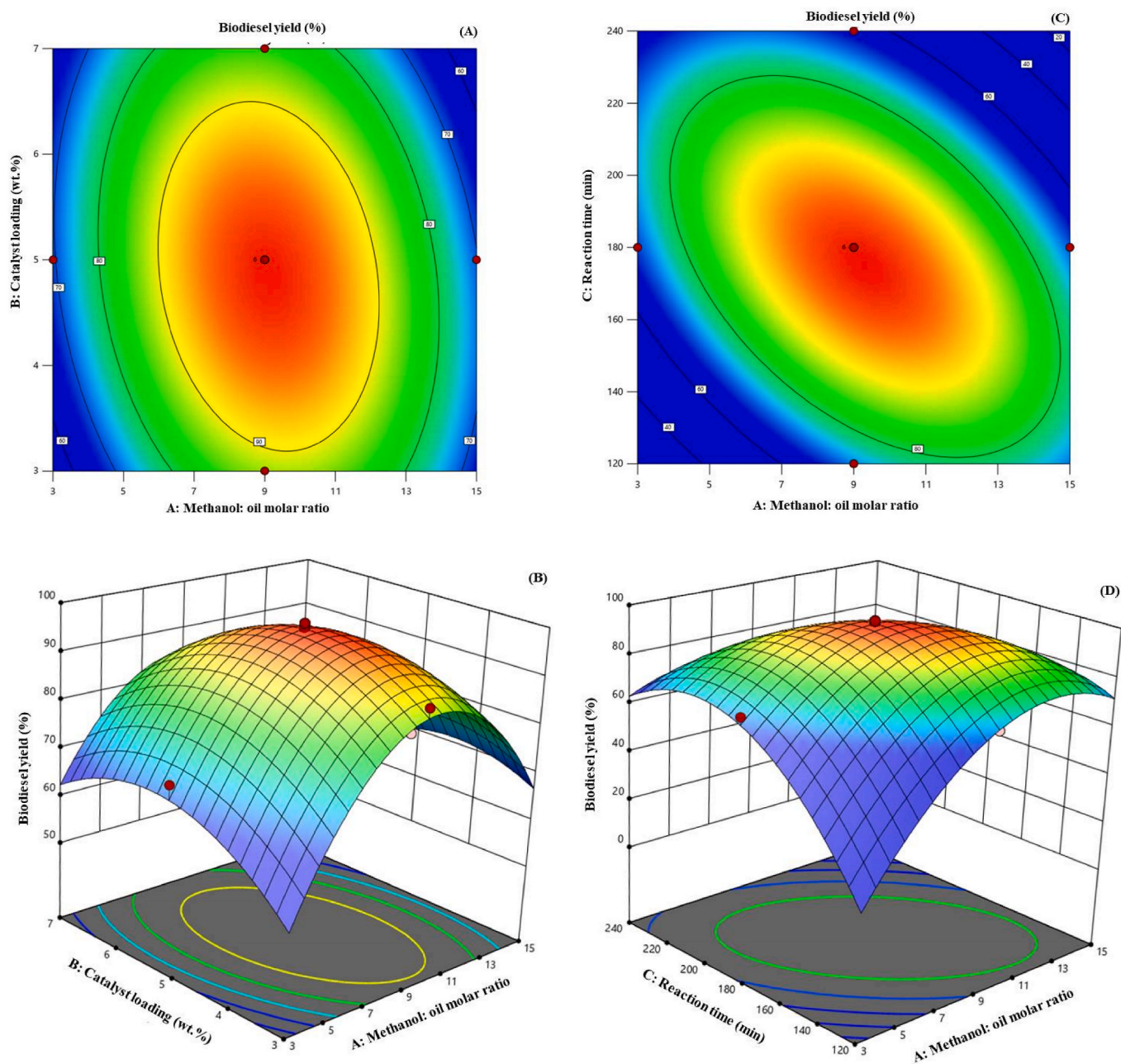
Fig. 1. Representative 2D contour plots and 3D response surfaces showing the interaction effect of (A, B) methanol: RPO molar ratio and catalyst loading, (C, D) methanol: RPO molar ratio and reaction time, and (E, F) catalyst loading and reaction time on biodiesel yield.

resulted in a biodiesel yield of over 98%. Interestingly, excessively high levels of catalyst caused saponification, which decreased the biodiesel yield. This effect is believed to be caused by increased mass transfer resistance in the reaction system [12,39]. There was no significant combined effect of the catalyst loading level and reaction time.

3.6. Process optimization by RSM

The optimum condition for producing biodiesel was evaluated using RSM via a CCD. The maximum predicted biodiesel yield (97.42%) was obtained with a methanol: RPO molar ratio of 9.34:1, a catalyst loading of 4.87 wt%, a reaction time of 175 min, and a reaction temperature of 65 °C (Fig. 2). This model was developed through experimentation and analysis. To validate the accuracy of the optimization analysis,

transesterification was conducted using the optimized reaction parameters, giving an obtained biodiesel yield of 96.49%, which was reasonably close to the predicted optimal condition (97.42%). The small error between the optimization and validation results, which was only 0.93%, further demonstrated the adequacy of the model to accurately predict the response. The present study achieved a higher biodiesel yield compared to the previously published 93.64% at a methanol: oil molar ratio of 4.1:1, a reaction temperature of 38 °C, and a reaction time of 30 h [40]. Likewise, biodiesel production from okra seed-based waste transesterification achieved an optimal biodiesel yield of 90.17% using a methanol: oil molar ratio of 30:1, 4.5 wt% catalyst, and a reaction time of 30 min at 70 °C [41]. In another study, a maximum biodiesel yield of 93% was achieved using a catalyst loading of 15 wt%, a methanol: oil molar ratio of 8:1, and a reaction temperature of 35 °C [42].
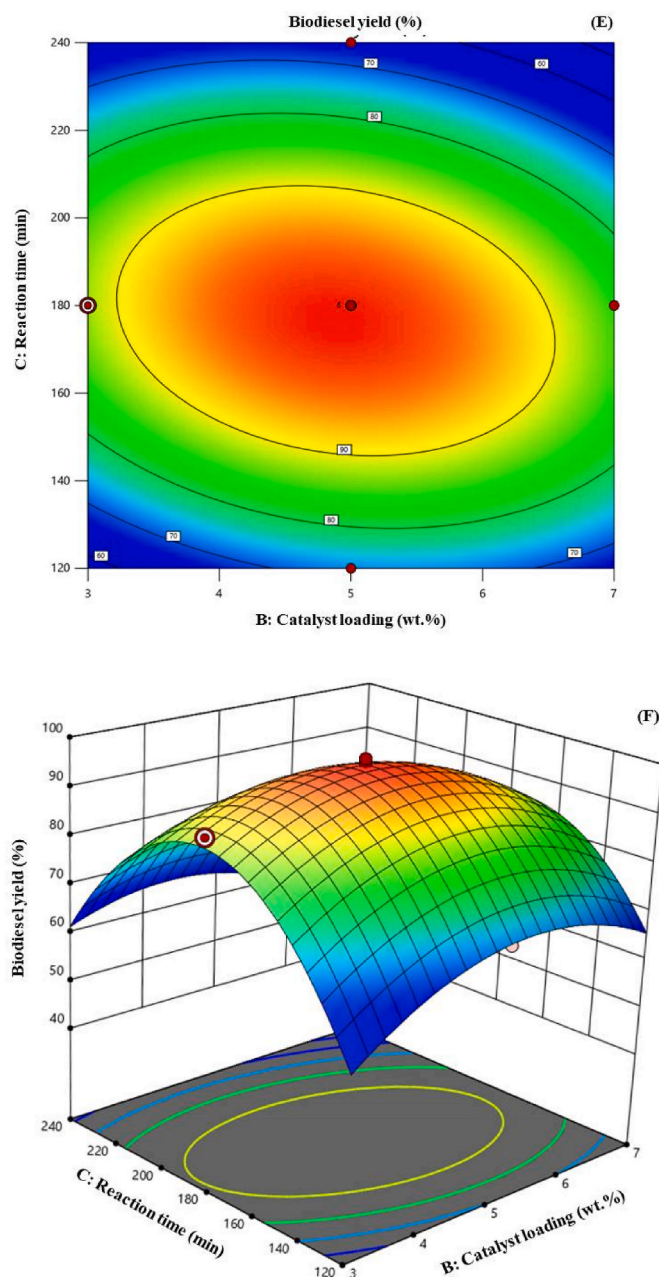
Fig. 1. (*continued*).

3.7. Reusability of the 35CaO/RSA-600 catalysts

The reusability of heterogeneous catalysts is essential for their practical application in biodiesel production. 35CaO/RSA-600 catalyst was evaluated for its reusability under optimal reaction conditions (see supplementary material). The study found that the catalyst demonstrated high catalytic activity of 96.49% in the first reaction cycle. However, over subsequent cycles, the biodiesel yield gradually decreased to 65.30% in the fifth cycle. This decrease in catalytic activity could be attributed to several factors. One possible factor is the loss of active sites due to deactivation. This means that the catalyst may no longer be able to perform its intended function due to a decrease in the number of active species available for the reaction to occur. Another potential factor is the formation of unwanted byproducts that may deposit on the catalyst surface [43]. This can lead to a reduction in the contact area between the oil and the catalyst active sites, which can further contribute to a decrease in catalytic activity [44]. Another factor

that could contribute to the decreasing activity of the catalyst is the partial leaching of calcium active species from the catalyst surface due to the repeated washing with methanol [45] can cause a significant decrease in the total basicity of the catalyst from the loss of active metal on the RSA support. In support in the fifth cycle, the total basicity and basic strength of the catalyst was found to be 3.10 mmol/g and $7.2 < H\_ < 9.8$, significantly lower than that in the first cycle.

3.8. FAME composition and fuel properties obtained using the 35CaO/RSA-600 heterogeneous catalyst

The FAME composition obtained after the transesterification of RPO with methanol using the 35CaO/RSA-600 catalyst under optimal conditions was mainly comprised of saturated fatty acids (SFAs), with C16:0 and C14:0 being the predominant ones (see supplementary material). The SFAs are known to increase the oxidative stability of biodiesel but can also lead to a higher viscosity and cloud point, which affects the
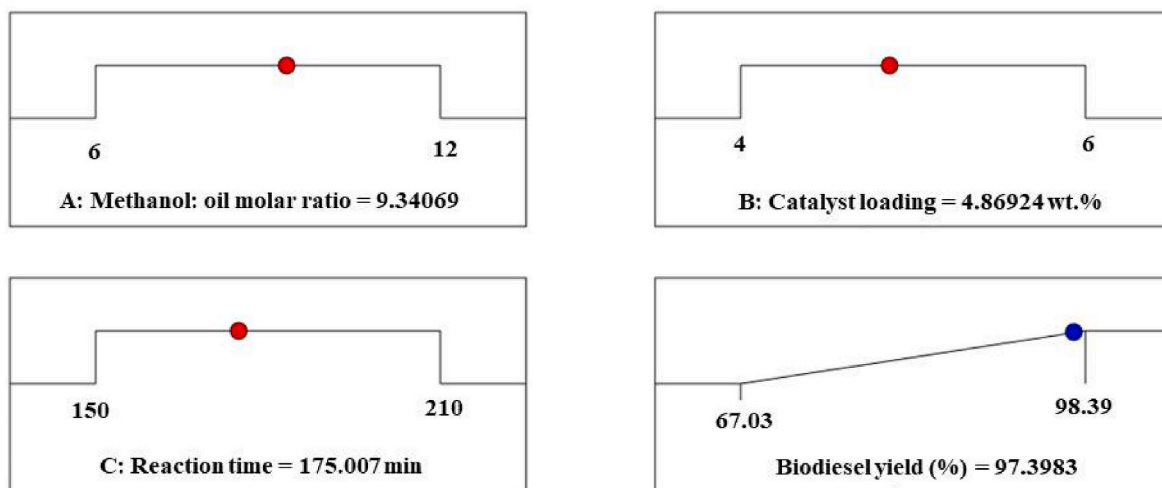
Fig. 2. Optimized values for the transesterification over the 35CaO/RSA-600 catalyst by RSM with CCD.

Table 5
Properties of obtained biodiesel using 35CaO/RSA-600 as heterogeneous catalyst.

Properties	ASTM D6751	EN 14214	This study
Ester content (%)	Not specified	96.5 min	96.49
Monoglycerides (wt%)	0.40 max	0.70 max	0
Diglycerides (wt%)	Not specified	0.20 max	0.15
Triglycerides (wt%)	Not specified	0.20 max	0.10
Density at 15 °C (kg/m³)	Not specified	860–900	876.3
Kinematic viscosity at 40 °C (mm²/s)	1.9–6.0	3.5–5.0	4.66

fuel's low-temperature operability [46]. The low levels of other SFAs, such as C17:0, C20:0, C22:0, and C24:0, are desirable since they have been reported to have negative effects on the cold flow properties of biodiesel. The monounsaturated fatty acid methyl esters (MUFA) present in the composition were *trans*-C16:1, *trans*-C18:1, and *cis*-C18:1, which have been shown to enhance the cold flow properties of biodiesel and improve its oxidative stability. The relatively high levels of *cis*-C18:1 is desirable since it has been reported to enhance the oxidative stability of biodiesel. The diunsaturated fatty acid methyl ester (DUFA) present in the FAME had a composition of C18:2. Overall, DUFAs are known to reduce the viscosity of biodiesel and improve its low-temperature properties [46].
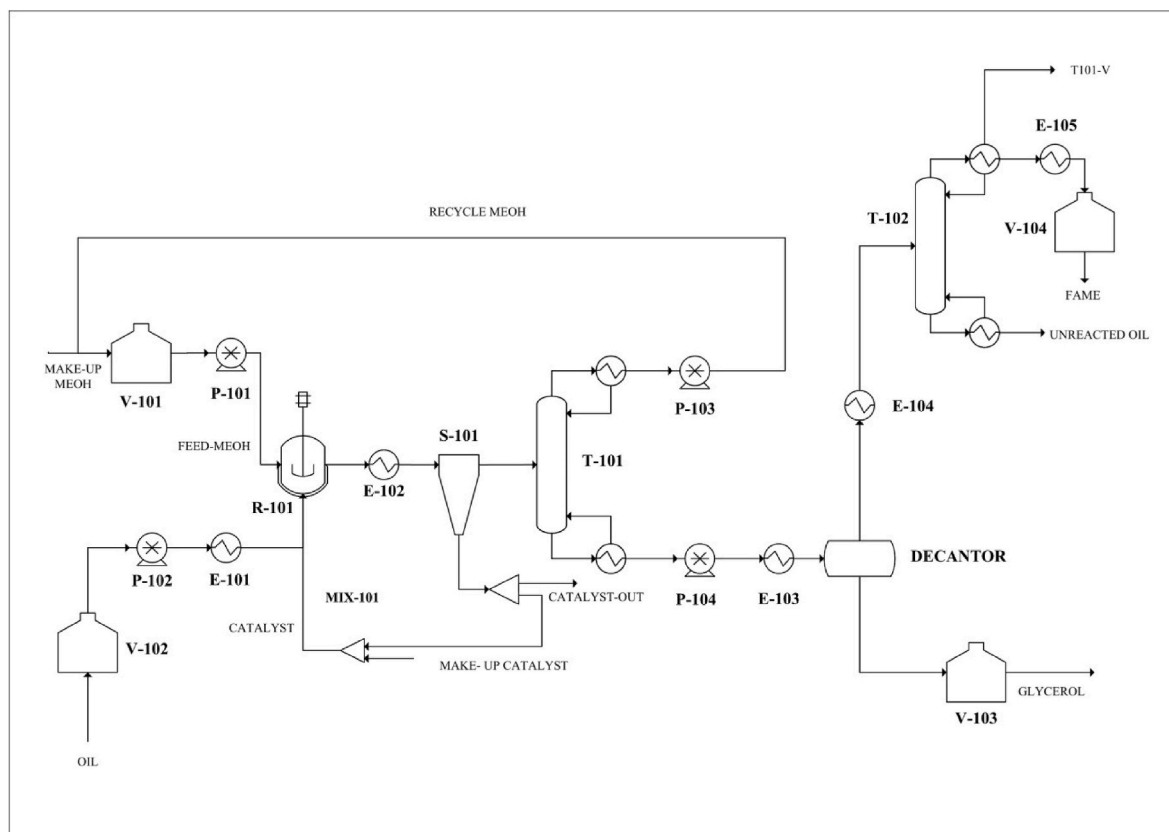

Fig. 3. Flow diagram of the biodiesel production process.

Table 6

Summary of results from major streams of a process flow diagram.

Stream	OIL	MKE-MEOH	FEED-MEOH	CATALYST	FAME	GLYCEROL
Temperature (°C)	25.00	25.00	48.50	29.25	25	25
Pressure (bar)	1.01	1.01	1.01	1.01	1.01	0.5
Molar flow (kmol/h)	1.27	4.37	12.59	0.98	3.65	1.76
Mass flow (kg/h)	1128.45	137.43	379.21	54.96	1079.93	126.49
Mass fractions						
Methanol	0.0000	0.9750	0.9683	0.0000	0.0002	0.0939
Triolein	1.0000	0.0000	0.0000	0.0000	0.0000	0.0002
Water	0.0000	0.0250	0.0317	0.0000	0.0000	0.0271
Glycerol	0.0000	0.0000	0.0000	0.0000	0.0005	0.8747
Methyl oleate	0.0000	0.0000	0.0000	0.0000	0.9992	0.0041
Catalyst	0.0000	0.0000	0.0000	1.0000	0.0000	0.0000

Table 7

Summary of equipment specifications and total equipment cost calculation (plant capacity: 10,000 ton/year).

Equipment	Specification	Size	Equipment cost (M$)
Storage tank			
V-101	4 days storage	V = 47.21 m³	0.223
V-102	capacity	V = 117.86 m³	0.128
V-103		V = 119.21 m³	0.258
V-104		V = 9.92 m³	0.102
Reactor			
R-101	3 h residence time	V = 7.00 m³	0.114
Distillation columns			
T-101	N = 5, N_F = 3, RR = 2	D_c = 0.39 m	0.006
		H_c = 2.93 m	
T-102	N = 5, N_F = 3, RR = 2	D_c = 2.16 m	0.052
		H_c = 4.39 m	
Heat exchangers			
E−101	U = 0.5 kW/(m² K)	A = 0.43 m²	0.024
E−102	U = 0.5 kW/(m² K)	A = 4.08 m²	0.059
E−103	U = 0.5 kW/(m² K)	A = 2.40 m²	0.043
E−104	U = 0.5 kW/(m² K)	A = 0.43 m²	0.016
E−105	U = 0.5 kW/(m² K)	A = 2.65 m²	0.046
T-101	U = 0.5 kW/(m² K)	A = 9.33 m²	0.095
T-102	U = 0.5 kW/(m² K)	A = 2.70 m²	0.046
Reboilers			
T-101	U = 1 kW/(m² K)	A = 3.33 m²	0.052
T-102	U = 1 kW/(m² K)	A = 7.12 m²	0.081
Decanter	1 h residence time	V = 1.50 m³	0.027
Pumps			
P-101	75% efficiency	Q = 0.51 m³/h	0.029
P-102	75% efficiency	Q = 1.23 m³/h	0.048
P-103	75% efficiency	Q = 0.34 m³/h	0.023
P-104	75% efficiency	Q = 6.31 m³/h	0.124
Hydrocyclone			
S-101		Q = 8 gal/min	0.002
Vacuum system		P = 80 kPa, 10kPa	0.020
Total equipment cost			1.621

Table 8

Summary of economic analysis of biodiesel production.

Detail	Cost
Total capital investment	4,530,374 USD
Total direct cost (TDC)	3,451,713 USD
Total indirect cost (TIC)	862,928 USD
Working capital investment (WCI)	215,732 USD
Total production cost (TPC)	4,169,698 USD
Direct production	3,525,535 USD
Fixed charges	60,405 USD
Plant overhead	208,485 USD
General expenses (GE)	375,273 USD
NPV	4,151,905.61 USD
IRR	17.20%
Payback period	7.17 years

Fig. 4. Total production cost (TPC) of the studied biodiesel plant.

Legend:
- Raw materials: 65.51% (2,731.43 tUSD)
- Utilities: 11.00% (458.64 tUSD)
- Labor cost: 5.46% (227.61 tUSD)
- Maintenance and repairs:2.07% (86.29 tUSD)
- Waste treatment: 0.52% (21.57 tUSD)
- Local taxes: 1.03% (43.15 tUSD)
- Insurance: 0.41% (17.26 tUSD)
- Plant-overhead costs: 5% (208.48 tUSD)
- Administrative costs: 2% (83.39 tUSD)
- Distribution and selling costs: 2% (83.39 tUSD)
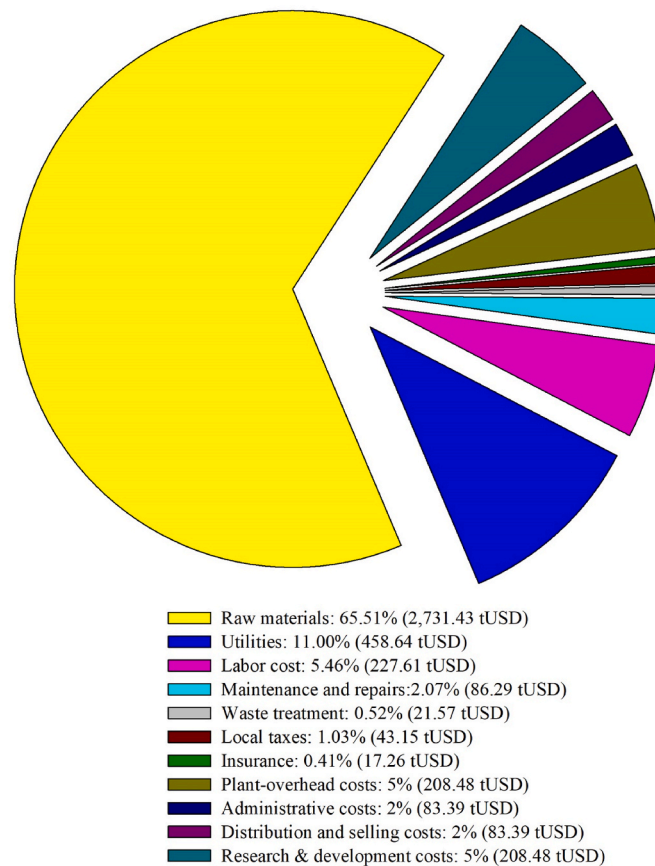- Research & development costs: 5% (208.48 tUSD)

In order for biodiesel to be a viable substitute for fossil diesel, it must adhere to stringent international standards of the European Norm (EN) and American Society for Testing Materials (ASTM). The fuel properties of the obtained biodiesel with the criteria specified in ASTM D6751 and EN 14,214 are shown in Table 5. Remarkably, the findings from this study demonstrate that all parameters of biodiesel analysis have successfully met the stringent standards as prescribed in ASTM D6751 and EN14214.

3.9. Process analysis

Fig. 3 depicts the biodiesel production process using the heterogeneous base-catalysis. The process commenced by blending fresh and
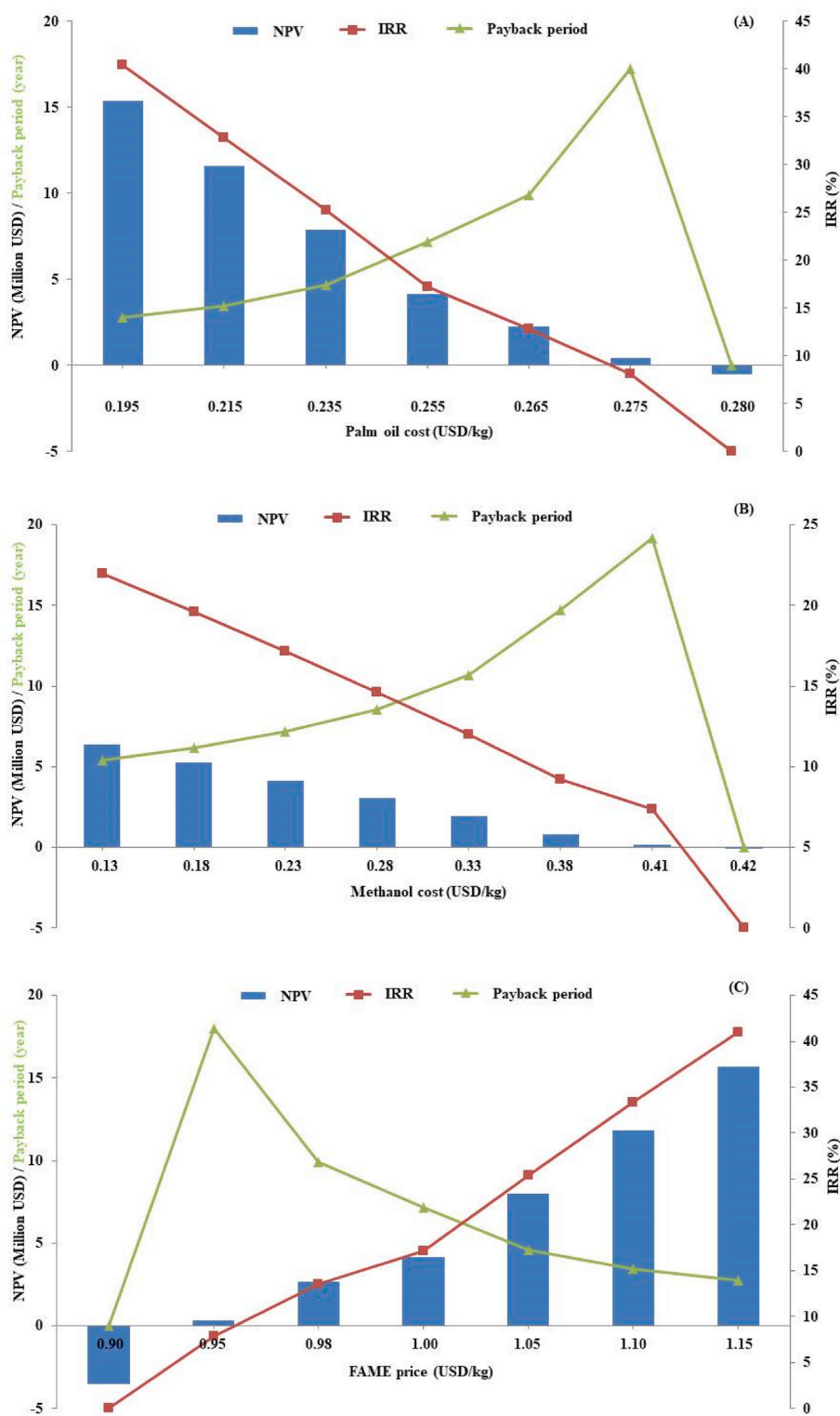
Fig. 5. Sensitivity analysis of the (A) RPO cost, (B) methanol cost, and (C) FAME price.

recycled methanol in a storage tank (V-101), followed by pumping it into reactor R-101, where it reacted with the preheated RPO in a stirred tank reactor. The optimum reaction condition was carried out with an RPO: methanol molar ratio of 9.34:1, catalyst loading level of 4.87 wt%, reaction temperature of 65 °C, and ambient pressure. These conditions led to a conversion rate of 96.49% within 175 minutes. The solid catalyst underwent separation from the liquid phase in a hydrocyclone (S-101) and was subsequently recycled back into R-101 at a split ratio of

0.85:0.15. Meanwhile, the liquid stream was directed to a distillation column (T-101) to recover the excess methanol, achieving a molar recovery rate of 94%. Methanol was collected as the distillate, while biodiesel and other components were collected at the bottom. The mixture of glycerol and biodiesel underwent separation in a decanter, with the phase enriched with FAME being directed to a multistage distillation column (T-102) for FAME purification under vacuum conditions. A small amount of unreacted oil was considered waste. The

summary of the stream results are shown in Table 6.

3.10. Economic study

3.10.1. The TPC

The purchased costs estimation of major equipment in the process model was determined using data obtained from process simulator (Table 7). The chemical engineering plant cost index (CEPCI) was used to update the equipment costs to the year 2023, as in Eq. (11):

$$C_{updated} = C_{reference} \times \frac{I}{I_{reference}} \tag{11}$$

where I is chemical engineering cost index (CEPCI index) in the year 2023 = 800.6 [47] and for $I_{reference}$ = 521.9 in the year 2009 [47].

A biodiesel plant can be a profitable business venture if the economic factors are carefully considered, with the TPC being a critical factor. According to a study, the estimated TPC for a biodiesel plant was 4,169,698 USD (Table 8). The study revealed that the raw materials category had the highest cost, accounting for 65.51% of the TPC (Fig. 4). Additionally, utilities accounted for 11.00% of the TPC, while labor costs were 5.46% of the TPC. The TPC also included other expenses, such as maintenance and repairs, waste treatment, local taxes, insurance, plant-overhead costs, administrative costs, distribution and selling costs, and research and development costs. These costs ranged from 0.41% to 5.00% of the TPC.

3.10.2. Benefits analysis

The financial analysis of the biodiesel production plant was evaluated in terms of three crucial financial metrics: NPV, IRR, and PBP (Table 8). Based on the results, the plant has a positive financial outlook. The NPV was determined to be 4,151,905.61 USD, signifying that the project is economically feasible and viable. A positive NPV implies that the investment is expected to generate profits that exceed the cost of capital, indicating a low risk of loss. The IRR was calculated to be 17.20%, which is the rate of return that equates the present value of the project's cash inflows with the present value of its cash outflows. This IRR is higher than the required rate of return, implying that the project is expected to be profitable. The PBP was estimated to be 7.17 years, which is the length of time required for the project to recover its initial investment. This PBP is within an acceptable range, indicating that the project has a relatively short PBP and is a financially prudent investment.

3.10.3. Sensitivity analysis

The financial feasibility of a biodiesel production plant is highly dependent on the raw material costs and the final product's selling price. Fluctuations in these costs can significantly impact the NPV, IRR, and PBP of the project.

This study considered a range of RPO prices from 0.195 to 0.280 USD/kg (Fig. 5A). As the RPO prices increased, the project's NPV decreased and the PBP lengthened. At 0.195 USD/kg, the project had a positive NPV of 15.36 million USD and a short PBP of 2.79 years. However, at 0.28 USD/kg, the project had a negative NPV of −0.52 million USD, indicating the potential lack of profitability.

Similarly, the study considered a range of methanol prices from 0.13 to 0.42 USD/kg (Fig. 5B). As the methanol prices increased, the project's NPV decreased and the PBP lengthened. At 0.42 USD/kg, the project had a negative NPV of −0.06 million USD, potentially rendering the investment unprofitable.

Conversely, the study showed that as FAME prices increased, the project's NPV increased and the PBP shortened (Fig. 5C). The study considered a range of FAME prices from 0.90 to 1.15 USD/kg. At 0.90 USD/kg, the project had a negative NPV of −3.53 million USD, and the PBP could not be determined.

4. Conclusions

This study aimed to optimize the conditions for sustainable biodiesel production from RPO while also considering the economic feasibility of the process. The low-cost biochar catalyst was synthesized from waste RS. Through experimentation, the 35CaO/RSA-600 catalyst was found to be the most suitable catalyst for biodiesel synthesis, with a sustainable biodiesel yield of 96.49%. The optimal conditions for biodiesel production were determined to be a methanol: RPO molar ratio of 9.34:1, catalyst loading level of 4.87 wt%, reaction time of 175 min, and a reaction temperature of 65 °C. The base case simulation of unit production cost gave a PBP of 7.17 years, an IRR of 17.20%, and an NPV value of 4,151,905.61 USD. It is important to note that changes in raw material and product costs can have a significant impact on the project's NPV, IRR, and PBP.

Declaration of competing interest

The authors declare that they have no known competing financial interests or personal relationships that could have appeared to influence the work reported in this paper.

Data availability

Data will be made available on request.

Appendix A. Supplementary data

Supplementary data to this article can be found online at https://doi.org/10.1016/j.cscee.2023.100432.

References

[1] M. Ahmed, K.A. Ahmad, D.V.N. Vo, M. Yusuf, A. Haq, A. Abdullah, M. Aslam, D. S. Patle, Z. Ahmad, E. Ahmad, M. Athar, Recent trends in sustainable biodiesel production using heterogeneous nanocatalysts: function of supports, promoters, synthesis techniques, reaction mechanism, and kinetics and thermodynamic studies, Energy Convers. Manag. 280 (2023), 116821.

[2] R. Manurung, S.Z.D.M. Parinduri, R. Hasibuan, B.H. Tarigan, A.G.A. Siregar, Synthesis of nano-CaO catalyst with SiO_2 matrix based on palm shell ash as catalyst support for one cycle developed in the palm biodiesel process, Case Stud. Chem. Environ. Eng. 7 (2023), 100345.

[3] K. Masera, A.K. Hossain, Advancement of biodiesel fuel quality and NO_x emission control techniques, Renew. Sustain. Energy Rev. 178 (2023), 113235.

[4] Y. Xie, D. Wang, S.F. Almojil, A.I. Almohana, A.F. Alali, Y. Zhou, A. Raise, CaO-$MgFe_2O_4@K_2CO_3$ as a novel and retrievable nanocatalyst for two-step transesterification of used frying oils to biodiesel, Process Saf. Environ. 172 (2023) 195–210.

[5] J.V.L. Ruatpuia, B. Changmai, A. Pathak, L.A. Alghamdi, T. Kress, G. Halder, A.E. H. Wheatley, S.L. Rokhum, Green biodiesel production from Jatropha curcas oil using a carbon-based solid acid catalyst: a process optimization study, Renew. Energy 206 (2023) 597–608.

[6] V. Aslan, T. Eryilmaz, Polynomial regression method for optimization of biodiesel production from black mustard (*Brassica nigra* L.) seed oil using methanol, ethanol, NaOH, and KOH, Energy 209 (2020), 118386.

[7] M.M. Naeem, E.G. Al-Sakkari, D.C. Boffito, E.R. Rene, M.A. Gadalla, F.H. Ashour, Single-stage waste oil conversion into biodiesel via sonication over bio-based bifunctional catalyst: optimization, preliminary techno-economic and environmental analysis, Fuel 341 (2023), 127587.

[8] M.A. Sundaramahalingam, P. Sivashanmugam, Concomitant strategy of wastewater treatment and biodiesel production using innate yeast cell (*Rhodotorula mucilaginosa*) from food industry sewerage and its energy system analysis, Renew. Energy 208 (2023) 52–62.

[9] G.N. Jham, B.R. Moser, S.N. Shah, R.A. Holser, O.D. Dhingra, S.F. Vaughn, M. A. Berhow, J.K. Winkler-Moser, T.A. Isbell, R.K. Holloway, E.L. Walter, R. Natalino, J.C. Anderson, D.M. Stelly, Wild Brazilian mustard (*Brassica juncea* L.) seed oil methyl esters as biodiesel fuel, J. Americ. Oil Chem. Soc. 86 (9) (2009) 917–926.

[10] S.S. Karkal, D.R. Rathod, A.S. Jamadar, S.S. Mamatha, T.G. Kudre, Production optimization, scale-up, and characterization of biodiesel from marine fishmeal plant oil using *Portunus sanguinolentus* crab shell derived heterogeneous catalyst, Biocatal. Agric. Biotechnol. 47 (2023), 102571.

[11] S. Brahma, B. Basumatary, S.F. Basumatary, B. Das, S. Brahma, S.L. Rokhum, S. Basumatary, Biodiesel production from quinary oil mixture using highly efficient *Musa chinensis* based heterogeneous catalyst, Fuel 336 (2023), 127150.

[12] B. Maleki, B. Singh, H. Eamaeili, Y.K. Venkatesh, S.S.A. Talesh, S. Seetharaman, Transesterification of waste cooking oil to biodiesel by walnut shell/sawdust as a novel, low-cost and green heterogeneous catalyst: optimization via RSM and ANN, Ind. Crops Prod. 193 (2023) 116261.

[13] M.Z. Yameen, H. AlMohamadi, S.R. Naqvi, T. Noor, W.H. Chen, N.A.S. Amin, Advances in production & activation of marine macroalgae-derived biochar catalyst for sustainable biodiesel production, Fuel 337 (2023), 127215.

[14] T. Silalertruksa, S.H. Gheewala, M. Sagisaka, K. Yamaguchi, Life cycle GHG analysis of rice straw bio-DME production and application in Thailand, Appl. Energy 112 (2013) 560–567.

[15] R. Li, Integrating the composition of food waste into the techno-economic analysis of waste biorefineries for biodiesel production, Bioresour. Technol. Rep. 20 (2022), 101254.

[16] R. Naveenkumar, G. Baskar, Process optimization, green chemistry balance and technoeconomic analysis of biodiesel production from castor oil using heterogeneous nanocatalyst, Bioresour. Technol. 320 (2021), 124347.

[17] J. Jitjamnong, C. Thunyaratchatanon, A. Luengnaruemitchai, N. Kongrit, N. Kasetsomboon, A. Sopajarn, N. Chuaykarn, N. Khantikulanon, Response surface optimization of biodiesel synthesis over a novel biochar-based heterogeneous catalyst from cultivated (*Musa sapientum*) banana peels, Biomass Conv. Bioref. 11 (6) (2021) 2795–2811.

[18] A.A. Albuquerque, F.T.T. Ng, L. Danielski, L. Stragevitch, Phase equilibrium modeling in biodiesel production by reactive distillation, Fuel 271 (2020), 117688.

[19] K. Gengiah, B. Gurunathan, N. Rajendran, J. Han, Process evaluation and techno-economic analysis of biodiesel production from marine macroalgae *Codium tomentosum*, Bioresour. Technol. 351 (2022), 126969.

[20] M.S. Peters, K.D. Timmerhaus, R.E. West, Plant Design and Economics for Chemical Engineers, fifth ed., McGraw-Hill chemical engineering series; McGraw-Hill, New York, 2003.

[21] M. Bhattacharya, M.K. Mandal, Synthesis of rice straw extracted nano-silica-composite membrane for CO₂ separation, J. Clean. Prod. 186 (2018) 241–252.

[22] C. Lin, W. Luo, T. Luo, Q. Zhou, H. Li, L. Jing, A study on adsorption of Cr (VI) by modified rice straw: characteristics, performances and mechanism, J. Clean. Prod. 196 (2018) 626–634.

[23] O. Sahu, Characterisation and utilization of heterogeneous catalyst from waste rice-straw for biodiesel conversion, Fuel 287 (2021), 119543.

[24] C. Zhao, L. Yang, S. Xing, W. Luo, Z. Wang, P. Lv, Biodiesel production by a highly effective renewable catalyst from pyrolytic rice husk, J. Clean. Prod. 199 (2018) 772–780.

[25] K. Qu, L. Huang, S. Hu, C. Liu, Q. Yang, L. Liu, K. Li, Z. Zhao, Z. Wang, TiO₂ supported on rice straw biochar as an adsorptive and photocatalytic composite for the efficient removal of ciprofloxacin in aqueous matrices, J. Environ. Chem. Eng. 11 (2) (2023), 109430.

[26] F. Ashine, Z. Kiflie, S.V. Prabhu, B.Z. Tizazu, V. Varadharajan, M. Rajasimman, S. W. Joo, Y. Vasseghian, M. Jayakumar, Biodiesel production from *Argemone*

[27] mexicana oil using chicken eggshell derived CaO catalyst, Fuel 332 (2023), 126166.

[27] A.A. El-sherif, A.M. Hamad, E. Shams-Eldin, H.A.A.E. Mohamed, A.M. Ahmed, M. A. Mohamed, Y.S. Abdelaziz, F.A.Z. Sayed, E.A.A. El qassem Mahmoud, T.M. Abd El-Daim, H.M. Fahmy, Power of recycling waste cooking oil into biodiesel via green CaO-based eggshells/Ag heterogeneous nanocatalyst, Renew. Energy 202 (2023) 1412–1423.

[28] S.G. Khan, M. Hassan, M. Anwar, Zeshan, U.M. Khan, C. Zhao, Mussel shell based CaO nano-catalyst doped with praseodymium to enhance biodiesel production from castor oil, Fuel 330 (2022), 125480.

[29] G.Y. Chen, R. Shan, J.F. Shi, B.B. Yan, Transesterification of palm oil to biodiesel using rice husk ash-based catalysts, Fuel Process. Technol. 133 (2015) 8–13.

[30] B. Basumatary, B. Das, B. Nath, S. Basumatary, Synthesis and characterization of heterogeneous catalyst from sugarcane bagasse: production of jatropha seed oil methyl esters, Curr. Res. Green Sustain. 4 (2021), 100082.

[31] S. Basumatary, B. Nath, B. Das, P. Kalita, B. Basumatary, Utilization of renewable and sustainable basic heterogeneous catalyst from *Heteropanax fragrans* (Kesseru) for effective synthesis of biodiesel from *Jatropha curcas* oil, Fuel 286 (2021), 119357.

[32] M. Pan, X. Gan, C. Mei, Y. Liang, Structural analysis and transformation of biosilica during lignocellulose fractionation of rice straw, J. Mol. Struct. 1127 (2017) 575–582.

[33] S. De, S. Mishra, E. Poonguzhali, M. Rajesh, K. Tamilarasan, Fractionation and characterization of lignin from waste rice straw: biomass surface chemical composition analysis, Int. J. Biol. Macromol. 145 (2020) 795–803.

[34] W. Cao, Z. Wang, Q. Zeng, C. Shen, ¹³C-NMR and XPS characterization of anion adsorbent with quaternary ammonium groups prepared from rice straw, corn stalk and sugarcane bagasse, Appl. Surf. Sci. 389 (2016) 404–410.

[35] M. Chhabra, B.S. Saini, G. Dwivedi, Optimization of the dual stage procedure of biodiesel synthesis from Neem oil using RSM based Box Behnken design, Energy Sources Part A (2020) 1–24.

[36] B. Basumatary, S. Basumatary, B. Das, B. Nath, P. Kalita, Waste *Musa paradisiaca* plant: an efficient heterogeneous base catalyst for fast production of biodiesel, J. Clean. Prod. 305 (2021), 127089.

[37] A. Arumugam, P. Sankaranarayanan, Biodiesel production and parameter optimization: an approach to utilize residual ash from sugarcane leaf, a novel heterogeneous catalyst, from *Calophyllum inophyllum* oil, Renew. Energy 153 (2020) 1272–1282.

[38] B. Dharmalingam, S. Balamurugan, U. Wetwatana, V. Tongnan, C. Sekhar, B. Paramasivam, K. Cheenkachorn, A. Tawai, M. Sriariyanun, Comparison of neural network and response surface methodology techniques on optimization of biodiesel production from mixed waste cooking oil using heterogeneous biocatalyst, Fuel 340 (2023), 127503.

[39] M. Rahimi, B. Aghel, M. Alitabar, A. Sepahvand, H.R. Ghasempour, Optimization of biodiesel production from soybean oil in a microreactor, Energy Convers. Manag. 79 (2014) 599–605.

[40] J. Iyyappan, J. Jayamuthunagai, B. Bharathiraja, A. Saravanaraj, R.P. Kumar, S. Balraj, Production of biodiesel from *Caulerpa racemosa* oil using recombinant *Pichia pastoris* whole cell biocatalyst with double displayed over expression of *Candida antartica* lipase, Bioresour. Technol. 363 (2022), 127893.

[41] R. Manimaran, M. Venkatesan, K.T. Kumar, Optimization of okra (*Abelmoschus esculentus*) biodiesel production using RSM technique coupled with GA: addressing its performance and emission characteristics, J. Clean. Prod. 380 (2022), 134870.

[42] A. Arumugam, D. Thulasidharan, G.B. Jegadeesan, Process optimization of biodiesel production from *Hevea brasiliensis* oil using lipase immobilized on spherical silica aerogel, Renew. Energy 116 (2018) 755–761.

[43] E. Betiku, A.A. Okeleye, N.B. Ishola, A.S. Osunleke, T.V. Ojumu, Development of a novel mesoporous biocatalyst derived from kola nut pod husk for conversion of *Kariya* seed oil to methyl esters: a case of synthesis, modeling and optimization studies, Catal. Lett. 149 (7) (2019) 1772–1787.

[44] A.S. Yusuff, A.O. Gbadamosi, L.T. Popoola, Biodiesel production from transesterified waste cooking oil by zinc-modified anthill catalyst: parametric optimization and biodiesel properties improvement, J. Environ. Chem. Eng. 9 (2) (2021), 104955.

[45] P.R. Pandit, M.H. Fulekar, Biodiesel production from microalgal biomass using CaO catalyst synthesized from natural waste material, Renew. Energy 136 (2019) 837–845.

[46] N.A. Amran, U. Bello, M.S.H. Ruslan, The role of antioxidants in improving biodiesel's oxidative stability, poor cold flow properties, and the effects of the duo on engine performance: a review, Heliyon 8 (7) (2022), e09846.

[47] Cost Indices, Chemical Engineering Plant Cost Index (CECPCI), 2023. https://to weringskills.com/financial-analysis/cost-indices/. (Accessed 6 June 2023).